Accepted Manuscript

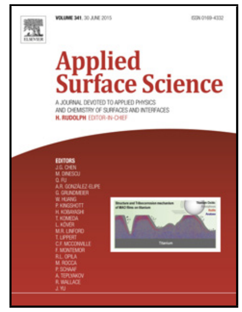

Title: Preparation, characterization, and nonlinear optical properties of hybridized graphene @ gold nanorods nanocomposites

Authors: Jia Guo, Tingyin Ning, Yanshun Han, Yingqiang Sheng, Chonghui Li, Xiaofei Zhao, Zhengyi Lu, Baoyuan Man, Yang Jiao, Shouzhen Jiang

PII:	S0169-4332(17)32965-3
DOI:	https://doi.org/10.1016/j.apsusc.2017.10.042
Reference:	APSUSC 37385
To appear in:	*APSUSC*
Received date:	23-5-2017
Revised date:	6-9-2017
Accepted date:	6-10-2017

Please cite this article as: Jia Guo, Tingyin Ning, Yanshun Han, Yingqiang Sheng, Chonghui Li, Xiaofei Zhao, Zhengyi Lu, Baoyuan Man, Yang Jiao, Shouzhen Jiang, Preparation, characterization, and nonlinear optical properties of hybridized graphene @ gold nanorods nanocomposites, Applied Surface Science https://doi.org/10.1016/j.apsusc.2017.10.042

Preparation, characterization, and nonlinear optical properties of hybridized graphene @ gold nanorods nanocomposites

Jia Guo [a], Tingyin Ning [a,b], Yanshun Han [c], Yingqiang Sheng [a], Chonghui Li [a], Xiaofei Zhao [a], Zhengyi Lu [a], Baoyuan Man [a], Yang Jiao [a], Shouzhen Jiang [a,b,*]

[a] *School of Physics and Electronics, Shandong Normal University, Jinan 250014, China*

[b] *Shandong provincial key laboratory of optics and photonic device, Shandong Normal University, Jinan 250014, China*

[c] *Qilu Institute of Technology, Jinan 250200, China*

Corresponding author.

E-mail addresses: jiang_sz@126.com (S. Jiang)

Highlights

- The methods of chemical vapor deposition (CVD) was used to obtain graphene. Compared with mechanical stripping, liquid phase stripping and epitaxial growth, graphene with high quality, large area and controllable number of layers can be prepared by CVD method. This makes it possible for us to obtain graphene with excellent nonlinear properties.
- We use a simple and inexpensive method to obtain the composite of graphene @ gold nanorods (G@GNRs). In addition, we used a simple method to measure the nonlinear optical properties of this material. This method provided the possibility for many budding teams to measure the nonlinear optical response of materials and to promote the development

of *Z*-scan technique.

- Compared with single graphene and GNRs, the G@GNRs nanocomposites exhibits many advantages, mainly including the following three aspects. First, the GNRs have better electron accepting ability compare with graphene. Therefore, compare with pristine graphene, the G@GNRs nanocomposites have more pronounced energy transfer effect. The significant energy transfer effect from GNRs to graphene is beneficial to enhance nonlinear optical response of the hybrid system; Second, the local electric field near the gold nanorods can be enlarged due to the surface plasmon resonance (SPR) effect, which can significantly enhance the nonlinear optical response of the G@GNRs nanocoposites. Further, the SPR wavelength of GNRs is tunable by varying the aspect ratio of GNRs, therefore, the strong nonlinear optical response of the G@GNRs nanocomposites can also be tuned in a wide range, which has important potential applications in nonlinear optical devices; Third, graphene is tightly attached to the surface of GNRs, which helps to enhance the oxidation resistance of the G@GNRs nanocomposites.

Abstract

The methods of chemical vapor deposition (CVD) and seed-mediated growth were used to obtain graphene and gold nanorods (GNRs), respectively. We fabricate graphene @ gold nanorods (G@GNRs) nanocomposites by successively using dropping and transferring methods. Through SEM, Raman spectra and TEM analysis, the number of graphene layers is 6-7. The diameter of gold nanorods (GNRs) is about 10 nm and the average aspect ratio is 6.5. In addition, we systematically investigate their nonlinear optical responses by using open-aperture *Z*-scan technique. In contrast with graphene and GNRs, the G@GNRs nanocomposites exhibit excellent nonlinear optical response with a modulation depth of about 51% and a saturable intensity of about 6.23 GW/cm^2. The results suggest that the G@GNRs nanocomposites could potentially be used as an optical modulator in pulsed laser generation.

Keywords: graphene; gold nanorods; nanocomposites; nonlinear optical responses; open-aperture *Z*-scan technique.

1. Introduction

Graphene, a layer of 2D sp^2-bonded carbon atoms, has been found to exhibit unique optical, electronic, thermal and mechanical properties [1-3]. These excellent properties of graphene make it as a promising material and have attracted a lot of scientific interest in various fields. The remarkable nonlinear optical properties of graphene have also attracted research interest of many groups and have been demonstrated in many reports [4-9]. The researchers found that graphene has excellent nonlinear optical properties due to extended π-conjugate system, the nonlinear scattering, two-photon absorption and the linear dispersion relation holding for its electronic band structure [10-14]. In recent years, many studies have shown that compared with the single component, the nanocomposites based on graphene and its derivatives (including covalently or noncovalently) can improve the nonlinear optical properties. For example, Jiang et al. fabricated MoS_2/graphene nanocomposites and found that the MoS_2/graphene nanocomposites possess lower saturable intensity and higher modulation depth comparing with single graphene [15]; Zhu et al. found that covalently functionalized graphene oxide and zinc phthalocyanine hybrid system has higher nonlinear optical extinction coefficients than those in graphene oxide [16]; Sakho et al. reported that graphene oxide noncovalent functionalized with silver nanoparticle have the higher reverse saturable absorption and lower saturable intensity comparing with the reduced graphene oxide [17]; Zheng et al. found that graphene oxide/Au hybrids doped organically modified silica gel glasses have more remarkable nonlinear optical properties [18]. Therefore, graphene can be combined with other materials to obtain composites with more excellent nonlinear optical properties.

Gold nanorods (GNRs) have attracted great interest due to their anisotropic splitting of the surface plasmon resonance into two polarization dependent components [19-21]. Compared with the weak transverse surface plasmon resonance (TSPR), the longitudinal surface plasmon resonance (LSPR) of GNRs can produce strong photoluminescence, scattering, absorption, and local-field enhancement. So GNRs has been widely utilized in many fields, such as biological imaging and sensing, photothermal therapy, optical data encoding, surface-enhanced Raman scattering and so on [22-24].

In recent years, many attempts have been made to synthesize hybrid systems of graphene and GNRs. This composite have been widely used in the fields of biosensors, electrochemical sensing, surface-enhanced Raman scattering, drug delivery, as well as others [25-31]. Although experimentalists have shown great interests in other properties of graphene and GNRs nanocomposites, their nonlinear optical properties remain unexplored. In our work, we use a simple and inexpensive method to obtain the composite of graphene@gold nanorods (G@GNRs). We have systematically studied the nonlinear optical properties of the G@GNRs through the open-aperture Z-scan system. Compared with single graphene and GNRs, the G@GNRs nanocomposites exhibits many excellent properties, mainly including the following three aspects. First, the GNRs have better electron accepting ability compare with graphene. Therefore, compare with pristine graphene, the G@GNRs nanocomposites have more pronounced energy transfer effect. The significant energy transfer effect from GNRs to graphene is beneficial to enhance nonlinear optical response of the hybrid system [32]; Second, the local electric field near the gold nanorods can be enlarged due to the surface plasmon resonance (SPR) effect, which can significantly enhance the nonlinear optical response of the G@GNRs nanocoposites [33]. Further, the SPR wavelength of GNRs is tunable by varying the aspect ratio of GNRs, therefore, the strong nonlinear optical response of the G@GNRs nanocomposites can also be tuned in a wide range, which has important potential applications in nonlinear optical devices [34]; Third, graphene is tightly attached to the surface of GNRs, which helps to enhance the oxidation resistance of the G@GNRs nanocomposites. The remarkable nonlinear optical properties and strong nonlinear optical response of the G@GNRs nanocomposites indicate that it has the potential to act as an optical modulator in pulsed laser generation.

2. Experiments

2.1. Preparation of graphene

The high-quality few layers graphene were fabricated on Cu foils by chemical vapor deposition (CVD) technology. The whole growth process can be divided into four steps. First, a high-purity Cu foil (99.999%, size of 10 × 10 cm^2) is put into the quartz tube in the tube furnace. Then, by using the double-pump system (mechanical pump and molecular pump), the pressure in the quartz tube was pumped to 10^{-3} Pa. Third, the gas mixture of CH_4 and H_2 was flowed-in the quartz tube to support graphene growth. The flow rates of CH_4 and H_2 are both 50 sccm. The growth temperature and time are 1000℃ and 30 min, respectively. Finally, by opening furnace lid, the temperature of the quartz tube was fast cooled down to room temperature with steadily flowing H_2 at rate of 15 sccm. Through the above steps, the graphene film was grown on Cu foil.

2.2. Preparation of GNRs

GNRs were synthesized through seed-mediated growth method [35,36]. First, 10 ml hexadecyltrimethyl ammonium bromide (0.2 M) was mixed with 10 ml $HAuCl_4$ (0.5 mM) and 1 ml $NaBH_4$ (0.01 mM) solution in a flask to form the seed solution. Then, the growth solution was obtained by mixing 20 ml hexadecyltrimethyl ammonium bromide (0.15 M), 12.5 ml 5-bromosalicylic acid (0.2 M) and 2 ml $AgNO_3$ aqueous solution (4 mM) with 1 ml ascorbic acid (0.1 mM) in a beaker. Finally, 0.5 ml of the seed solution was added into the growth solution. In order to make sure of the full growth of GNRs, the final solution was kept for 48 h at room temperature.

2.3. Preparation of G@GNRs

The diagram of synthesis G@GNR nanocomposites is shown in Fig. 1. First, the prepared GNRs solution was uniformly deposited on the mica substrate by using a spin-coating method with 2000 rmp rotating speed. After that, the mica substrate with GNRs solution was dried at room temperature. Second, the Cu foil with graphene was etched by 0.5 M $FeCl_3$ aqueous solution. After etching, the graphene film floats on the surface of the $FeCl_3$ aqueous solution. In order to remove the remaining etchant, the graphene film was rinsed two times in deionized water. Third, the G@GNRs nanocomposites were obtained by using mica substrate with GNRs to scoop up the graphene floating on the surface of deionized water. Finally, the composite structure was dried at room temperature.

2.4. Apparatus and characterization

The Raman spectroscopy was obtained by using a Raman spectrometer with laser excitation at 532 nm (Horiba HR Evolution 800). Surface morphologies of the G@GNRs nanocomposites were observed by using a scanning electron microscopy (SEM, Zeiss Gemini Ultra-55). The transmission electron microscopy (TEM) was performed by using a transmission electron microscopy system (Hitachi H-800). Ultraviolet-uisible spectrophotometer (UV-Vis Spectrophotometer, U-4100) was used to collect UV-Vis absorption spectra.

3. Results and discussion

As shown in Fig. 2(a), by the virtue of the spin-coating method, GNRs were uniformly deposited on the mica substrate. The uniform GNRs enable the substrate to have well-ordered structure for Z-Scan. Figure 2(b) shows the SEM image of the graphene films on the mica substrate. In order to further prove the existence of graphene films, the Raman spectra from the substrate was measured, as shown in Fig. 2(c). We can clearly observed the D, G and 2D peaks of graphene at 1360, 1580 and 2695 cm^{-1}, respectively. By analyzing the intensity ratio between the 2D band and the G band, the ratio of I_{2D}/I_G corresponding to the few-layer (6-7 layers) graphene [37,38]. Besides, the defect related D peak is very weak, indicating that graphene grown by CVD method has high quality. As shown in Fig. 2(d), SEM image of the

G@GNRs films on the mica substrate was clearly observed. By contrast with Fig. 2(a), we can clearly see the silk like graphene attached to the GNRs. Besides, the GNRs on the G@GNRs substrate still maintains the well-ordered structure, which enhances the homogeneity of the G@GNRs substrate.

In order to demonstrate the preparation of GNRs, graphene and G@GNRs, the GNRs, graphene and G@GNRs were further characterized, as shown in Fig. 3. As shown in Fig. 3(a), the surface morphologie of GNRs were characterized by TEM. The inset of Fig. 3(a) shows their aspect ratio distribution with an average aspect ratio of 6.5. The relatively concentrated aspect ratio distribution indicates that the size of gold nanorods is very homogeneous. Figure 3(b) shows the UV-Vis absorption spectra of the aqueous solution of GNRs. The GNRs aqueous solution has two absorption peaks at 532 and 1060 nm, respectively. The absorption peak at 532 nm was caused by the TSPR of GNRs. The other one peak at 1060 nm was caused by the LSPR of GNRs. In order to observe more clearly, the HRTEM image of the GNRs was obtained, as shown in Fig. 3(c). The diameters of the GNRs are about 10 nm. In addition, through this image we can see the lattice fringes of the GNRs, indicating the high quality of the GNRs. In Fig. 3(d), a typical HRTEM image of the graphene films measured at the sample after transferring from the Cu foils to a copper grid for TEM examination is presented. The thickness of graphene films is 2.41 nm in the position of the red arrows, which indicates the number of graphene layers is seven since the interlayer spacing of graphene film is 0.34 nm [39]. Figure 3(e) shows the TEM image of the G@GNRs nanocomposites. We can see from the image that graphene films are attached to the GNRs to form the G@GNRs nanocomposites. The HRTEM image of the G@GNRs nanocomposites was obtained, as shown in Fig. 3(f). From the red circle in Fig. 3(f), the interface between graphene and GNRs can be clearly observed.

The open-aperture *Z*-scan technique was used to investigate the nonlinear optical properties of the prepared G@GNRs nanocomposites. The detailed light path is shown in Fig. 4. The sample is irradiated by picosecond pulses from a picosecond laser (center wavelength: 1064 nm, repetition rate: 1 Hz, pulse duration: 30 ps). By using a optical attenuator, the average power can be artificially controlled to ensure that the incident laser power is lower than the optical damage threshold of the sample. We used a beam splitter to separate 50% of the incident laser beam. This 50% incident laser is measured by detector 1 as a reference of the optical power. Another 50% incident laser is focused by a lens with a focal length of 150cm and generating a waist radius of 50 μm. The G@GNRs nanocomposites is perpendicular to the beam axis and shifted along the *Z*-axis via a linear electric platform. Then all the light passing through the G@GNRs nanocomposites was measured by detector 2. The optical power of Detector 1 and Detector 2 are measured simultaneously by computer controlled dual-channel power meter.

Experimental results of the open-aperture Z-scan measurements are shown in Fig. 5. The open-aperture curves of normalized transmittance all exhibit symmetric peak patterns around the focal point (z = 0), which indicate the existence of nonlinear saturable absorption in all the samples we prepared. In contrast with GNRs and graphene, the G@GNRs nanocomposites exhibit larger transmittance values with the same input intensity (265 GW/m^2) on the focus, indicating an enhanced light-matter interaction compared with that in GNRs or graphene. In order to quantitatively determine the nonlinear optical properties of the GNRs, graphene and G@GNRs, we using the Z-scan theory to process Z-scan data. According to the Z-scan theory, the open-aperture Z-scan curves in Fig. 5 was fitted by using the following equation [15]:

$$T\,(Z) = \left(1 - \frac{\alpha_0 L I_s}{I_s + I_0/(1+Z^2/Z_0^2)}\right)/(1-\alpha_0 L) \quad (1)$$

where Z is the sample position relative to the focus position, Z_0 is the diffraction length of the beam, $\alpha_0 L$ is the modulation depth, $T\,(Z)$ is the normalized transmittance at Z, I_0 is peak onaxis intensity at focus and I_s is the saturable intensity. The modulation depth of the GNRs, graphene and G@GNRs are obtained according to the linear optical transmittance at 1064 nm, as shown in Fig. 5(d). By fitting the experimental data, we obtained the saturable intensity of the GNRs, graphene and G@GNRs, which are shown in Table 1. In order to obtain the nonlinear absorption coefficient, we use the following equation [40]:

$$T\ (Z) = 1 - \frac{\beta I_0 L_{eff}}{2\sqrt{2}(1+Z^2/Z_0^2)} \quad (2)$$

where $L_{eff} = (1 - e^{-\alpha_0 L})/\alpha_0$ is the effective length, α_0 is the linear absorption coefficient, and β is the nonlinear absorption coefficient. The values of linear absorption coefficient and nonlinear absorption coefficient are shown in Table 1.

By fitting the experimental data, the nonlinear optical properties of the GNRs, graphene and G@GNRs was obtained, as shown in Table 1. In contrast with GNRs and graphene, the G@GNRs nanocomposites have lower saturable intensity, larger higher nonlinear absorption coefficient and higher modulation depth. This phenomenon can be attributed to the nonlinear scattering, free-carrier absorption and excited-state absorption[18]. Compare with graphene, the GNRs have better electron accepting ability. So more pronounced energy transfer effect was seen in the the G@GNRs nanocomposites comparing with pristine graphene. The energy transfer effect from GNRs to graphene enhances the nonlinear optical response of the hybird system. In addition, the SPR effect endows the gold nanorods a large local electric field, which can significantly enhance the nonlinear optical response of the G@GNRs nanocoposites. To investigate the laser radiation stability of the G@GNRs nanocomposites, we kept the laser radiation on the samples for two hours, and measured the opitcal transmittance every 20 minutes, as shown in the Fig. 6. The shadow area represents the vibration range of the transmittance. The black line in the shaded area is the average transmittance. All the values of the transmittance lie within a 4.9% variation range, which reveals the excellent laser radiation stability of the G@GNRs nanocoposites. Due to G@GNRs nanocomposites have excellent nonlinear optical properties, it can be considered as a nonlinear optical material for ultrafast photonics applications. Further studies of the G@GNRs nanocomposites as saturable absorbers for passive mode-locking laser are now in progress in our group.

4. Conclusions

The G@GNRs nanocomposites were prepared by successively using dropping and transferring methods. The nanostructure and morphology of the G@GNRs nanocomposites were investigated by SEM, Raman spectra and TEM analysis. By performing open-aperture Z-scan measurement, it has been found that the G@GNRs nanocomposites shows remarkable nonlinear optical response with a modulation depth of 51% and a saturable intensity of about 6.23 GW/cm^2. These results suggest that the G@GNRs nanocomposites are probably be developed as a saturable absorber for ultrafast photonics applications.

Funding

This work is supported by National Natural Science Foundation of China (NSFC) (Grant No. 11674199, 11474187, 11405098, 11404195, 61205174) and Excellent Young Scholars Research Fund of Shandong Normal University.

References

[1] M.J. Allen, V.C. Tung, and R.B. Kaner, Honeycomb carbon: a review of graphene, Chem. Soc. Rev. 110 (1) (2010) 132–145.
[2] C.N.R. Rao, A.K. Sood, K.S. Subrahmanyam, and A. Govindaraj, Graphene: the new two-dimensional nanomaterial, Angew. Chem. Int. Ed. 48 (42) (2009) 7752–7777.
[3] O.C. Compton and S.B.T. Nguyen, Graphene oxide, highly reduced graphene oxide, and graphene: versatile building blocks for carbon-based materials, Small 6 (6) (2010) 711–723.
[4] M.Feng, H.B. Zhan, and Y. Chen, Nonlinear optical and optical limiting properties of graphene families, Appl. Phys. Lett. 96 (3) (2010) 033107.
[5] E. Hendry, P. J. Hale, J. Moger, and A. K. Savchenko, Coherent nonlinear optical response of graphene, Phys. Rev. Lett. 105 (5) (2010) 212–217.
[6] B.J. Wang, Y. Hernandez, M. Lotya, J.N. Coleman, and W.J. Blau, Broadband nonlinear optical response of graphene dispersions, Adv. Mater. 21 (24) (2010) 2430–2435.
[7] G.K. Lim, Z.L. Chen, J.Clark, R.G.S. Goh, W.H. Ng, H.W. Tan, R.H. Friend, P.K.H. Ho, and L.L. Chua, Giant broadband nonlinear optical absorption response in dispersed graphene single sheets, Nat. Photonics 5 (9) (2011) 554–560.
[8] A.R. Wright, X.G. Xu, J.C. Cao, and C. Zhang, Strong nonlinear optical response of graphene in the terahertz regime, Appl. Phys. Lett. 95 (7) (2009) 666.
[9] K.L. Ishikawa, Nonlinear optical response of graphene in time domain, Phys. Rev. B 82 (20) (2010) 201402.
[10] L.L. Tao, B. Zhou, G.X. Bai, Y.G. Wang, S.F. Yu, S.P. Lau, Y.H. Tsang, J.Q. Yao, and D.G. Xu, Fabrication of covalently functionalized graphene oxide incorporated solid-state hybrid silica gel glasses and their improved nonlinear optical response, J. Phys. Chem. C 117 (44) (2013) 23108–23116.
[11] X.F. Jiang, L. Polavarapu, S.T. Neo, T. Venkatesan, and Q.H. Xu, Graphene

oxides as tunable broadband nonlinear optical materials for femtosecond laser pulses, J. Phys. Chem. Lett. 3 (6) (2012) 785–790.

[12] N. Liaros, P. Aloukou, A. Kolokithas-Ntoukas, A. Bakandritsos, T. Szabo, R. Zboril, and S. Couris, Nonlinear optical properties and broadband optical power limiting action of graphene oxide colloids, J. Phys. Chem. C 117 (13) (2013) 6842–6850.

[13] X.Q. Zheng, M. Feng, and H.B. Zhan, Giant optical limiting effect in Ormosil gel glasses doped with graphene oxide materials, J. Mater. Chem. C 1 (41) (2013) 6759–6766.

[14] Z.B. Liu, X.L. Zhang, Y.F. Xu, Y.S. Chen, and J.G. Tian, Nonlinear optical properties of graphene oxide in nanosecond and picosecond regimes, Appl. Phys. Lett. 94 (2) (2009) 021902.

[15] Y. Jiang, L. Miao, G. Jiang, Y. Chen, X. Qi, X. Jiang, H. Zhang, and S. Wen, Broadband and enhanced nonlinear optical response of MoS_2/graphene nanocomposites for ultrafast photonics applications, Sci. Rep. 5 (2015) 16372.

[16] J.H. Zhu, X.Y. Li, Y. Chen, J. Wang, C. Zhang, J.J. Zhang, and W.J. Blau, Graphene oxide covalently functionalized with zinc phthalocyanine for broadband optical limiting, Carbon 49 (6) (2011) 1900–1905.

[17] E.M. Sakho, O.S. Oluwafemi, P. Sreekanth, R. Philip, S. Thomas, N. Kalarikkal, Improved nonlinear optical and optical limiting properties in non-covalent functionalized reduced graphene oxide/silver nanoparticle (NF-RGO/Ag-NPs) hybrid, Opt. Mater. 58 *(2016)* 476–*483*.

[18] C. Zheng, W. Chen, S. Cai, X. Xiao, and X. Ye, Influence of doping level on the structure, texture, and nonlinear optical properties of graphene oxide/Au hybrids doped ORMOSIL gel glasses, Ceram. Int. 40 (10) *(2014)* 16245–*16251*.

[19] B. Nikoobakht and M.A. El-Sayed, Preparation and growth mechanism of gold nanorods (NRs) using seed-mediated growth method, Chem. Mater. 15 (10) (2003) 1957–*1962*.

[20] T.K. Sau and C.J. Murphy, Seeded high yield synthesis of short Au nanorods in aqueous solution, Langmuir 20 (15) (2004) 6414–*6420*.

[21] P. Zijlstra, J.W. M. Chon, and M. Gu, Five-dimensional optical recording mediated by surface plasmons in gold nanorods, Nature 459 (7245) (2009) 410.

[22] A. Bouhelier, R. Bachelot, G. Lerondel, S. Kostcheev, P. Royer, and G.P. Wiederrecht, Surface plasmon characteristics of tunable photoluminescence in single gold nanorods, Phys. Rev. Lett. 95 (26) (2005) 267405.

[23] L. Tong, Q.S. Wei, A. Wei, and J.X. Cheng, Gold nanorods as contrast agents for biological imaging: optical properties, surface conjugation and photothermal effects, Photochem. Photobiol. 85 (1) (2009) 21–*32*.

[24] X.H. Huang, S. Neretina, and M.A. El-Sayed, Gold nanorods: from synthesis and properties to biological and biomedical applications, Adv. Mater. 21 (48) (2009) 4880–4910.

[25] X. Fu, L. Chen, J.Li, M. Lin, H. You, and W. Wang, Label-free colorimetric sensor for ultrasensitive detection of heparin based on color quenching of gold nanorods by graphene oxide, Biosens. Bioelectron. 34 (1) (2012) 227–231.

[26] W. Li, J. Wang, J. Ren, and X. Qu, Near-infrared- and pH-responsive system for reversible cell adhesion using graphene/gold nanorods functionalized with i-motif DNA, Angew. Chem. Int. Edit. 52 (26) *(2013)* 6726–*6730.*

[27] H. Moon, D. Kumar, H. Kim, C. Sim, J.H. Chang, J.M. Kim, H. Kim, and D.K. Lim, Amplified photoacoustic performance and enhanced photothermal stability of reduced graphene oxide coated gold nanorods for sensitive photoacoustic imaging, ACS Nano **9** (3) (2015) 2711–2719.

[28] J. Zhang, Y. Sun, B. Xu, H. Zhang, Y. Gao, H. Zhang, and D. Song, A novel surface plasmon resonance biosensor based on graphene oxide decorated with gold nanorod–antibody conjugates for determination of transferrin, Biosens. Bioelectron. 45 (2013) 230–236.

[29] X. Han, X. Fang, A. Shi, J. Wang, and Y. Zhang, An electrochemical DNA biosensor based on gold nanorods decorated graphene oxide sheets for sensing platform, Anal. Biochem. 443 (2) (2013) 117–123.

[30] C. Hu, J. Rong, J. Cui, Y. Yang, L. Yang, Y. Wang, and Y. Liu, Fabrication of a graphene oxide–gold nanorod hybrid material by electrostatic self-assembly for surface-enhanced Raman scattering, Carbon 51 (2013) 255–264.

[31] U. Dembereldorj, S.Y. Choi, E.O. Ganbold, N.W. Song, D. Kim, J. Choo, S.Y. Lee, S. Kim, and S.W. Joo, Gold nanorod-assembled PEGylated graphene-oxide nanocomposites for photothermal cancer therapy, Photochem. Photobiol. 90 (3) (2014) 659–666.

[32] J. Wang, Y. Chen, R. Li, H. Dong, L. Zhang, M. Loty, J.N. Coleman, and W. J. Blau Nonlinear Optical Properties of Graphene and Carbon Nanotube Composites, Carbon Nanotubes-Synthesis, Characterization, Applications (2011).

[33] H. B. Liao, R. F. Xiao, J. S. Fu, P. Yu, G. K. L. Wong, and P. Sheng, Large third-order optical nonlinearity in Au:SiO2 composite films near the percolation threshold, Appl. Phys. Lett. 70 (1) (1997) 1-3.

[34] H. Chen, L. Shao, Q. Li, and J.Wang, Gold nanorods and their plasmonic properties, Chem. Soc. Rev. 42 (7) (2013) 2679-2724.

[35] X.C. Ye, L.H. Jin, H. Caglayan, J. Chen, G.Z. Xing, C. Zheng, V.D. Nguyen, Y.J. Kang, N. Engheta, C.R. Kagan, and C.B. Murray, Improved size-tunable synthesis of monodisperse gold nanorods through the use of aromatic additives, ACS Nano 6 (3) (2012) 2804–2817.

[36] X.C. Ye, C. Zheng, J. Chen, Y.Z. Gao, and C.B. Murray, Using binary surfactant mixtures to simultaneously improve the dimensional tunability and monodispersity in the seeded growth of gold nanorods, Nano Lett. 13 (2) (2013) 765–771.

[37] X.S. Li, W.W. Cai, J. An, S. Kim, J. Nah, D.X. Yang, R. Piner, A. Velamakanni, I. Jung, E. Tutuc, S.K. Banerjee, L. Colombo, and R.S. Ruoff, Large-area synthesis of high-quality and uniform graphene films on copper foils, Science 324 (5932) (2009) 1312–1314.

[38] S.C. Xu, B.Y. Man, S.Z. Jiang, C.S. Chen, C. Yang, M. Liu, X.G. Gao, Z.C. Sun, and C. Zhang, Direct synthesis of graphene on SiO_2 substrates by chemical

vapor deposition, CrystEngComm 15 (10) (2013) 1840–1844.

[39] T.T. Cao, V.C. Nguyen, H.B. Nguyen, H.T. Bui, T.T. Vu, N.H. Phan, B.T. Phan, L. Hoang, M. Bayle, M. Paillet, J.L. Sauvajol, N.M. Phan, and D.L. Tran, Fabrication of few-layer graphene film based field effect transistor and its application for trace-detection of herbicide atrazine, Adv. Nat. Sci.: Nanosci. Nanotechnol. 7 (3) (2016) 035007.

[40] T. Ning, C. Chen, Y, Zhou, H. Lu, D. Zhang, H. Ming, and G. Yang, Large optical nonlinearity in $CaCu_3Ti_4O_{12}$ thin films, Appl. Phys. A-Mater. 94 (3) (2009) 567–570.

Figures

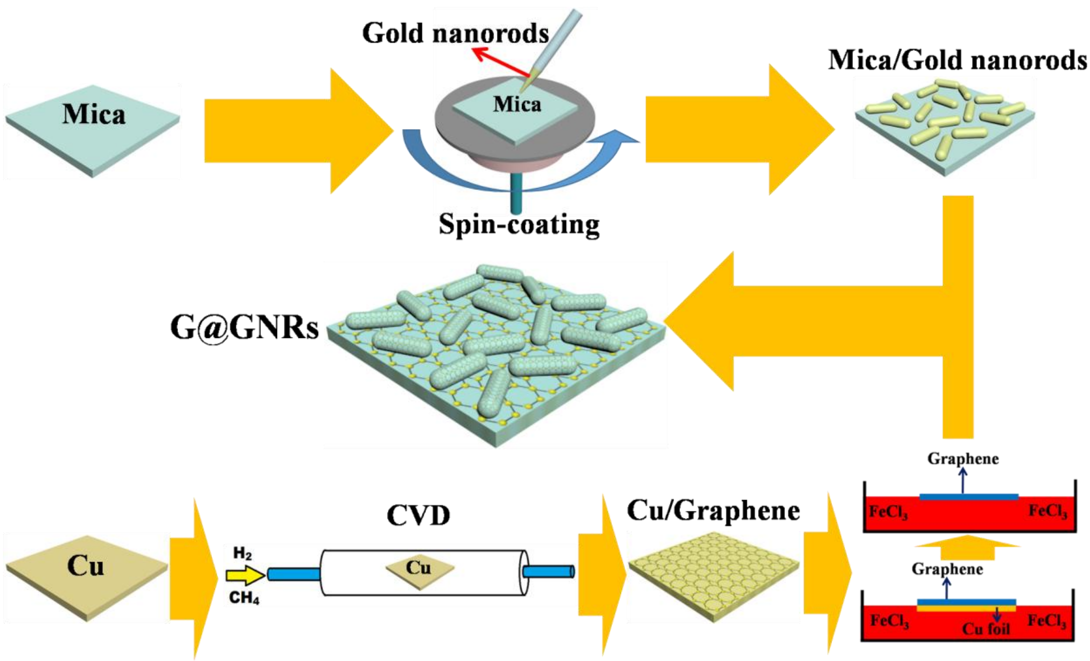

Fig. 1. Diagram of synthesis G@GNR nanocomposites.

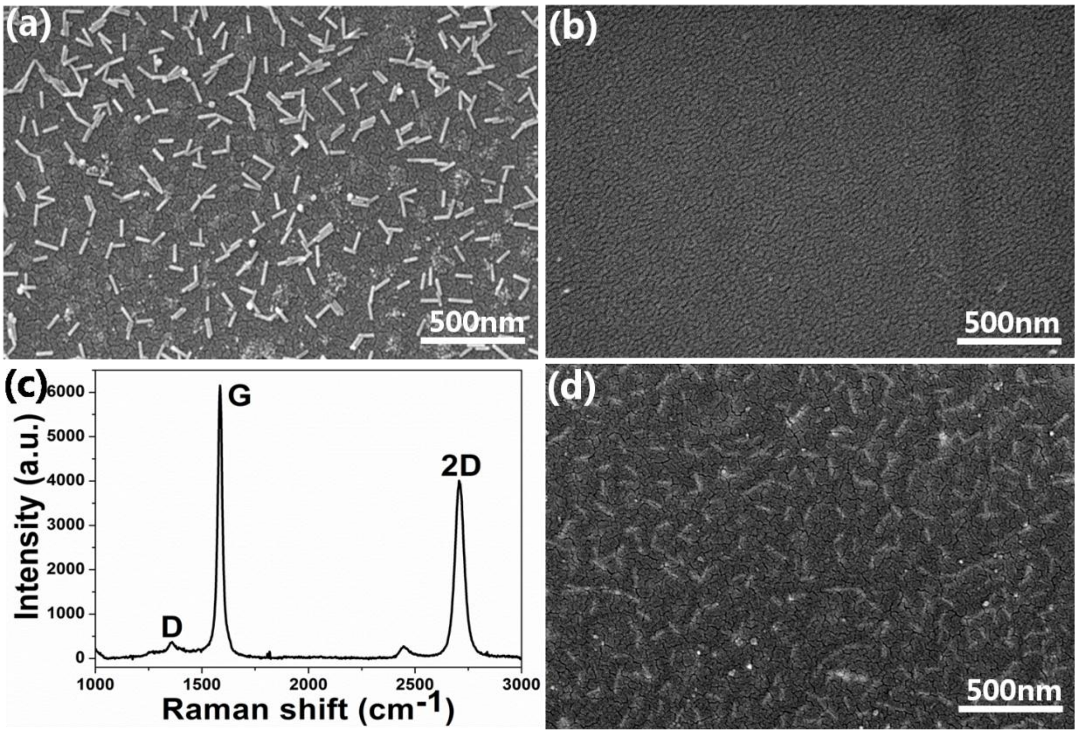

Fig. 2. (a) and (b) are SEM images of the GNRs and graphene films on the mica substrate, respectively. (c) Raman characterization of the graphene films. (d) SEM image of the G@GNRs nanocomposites on the mica substrate.

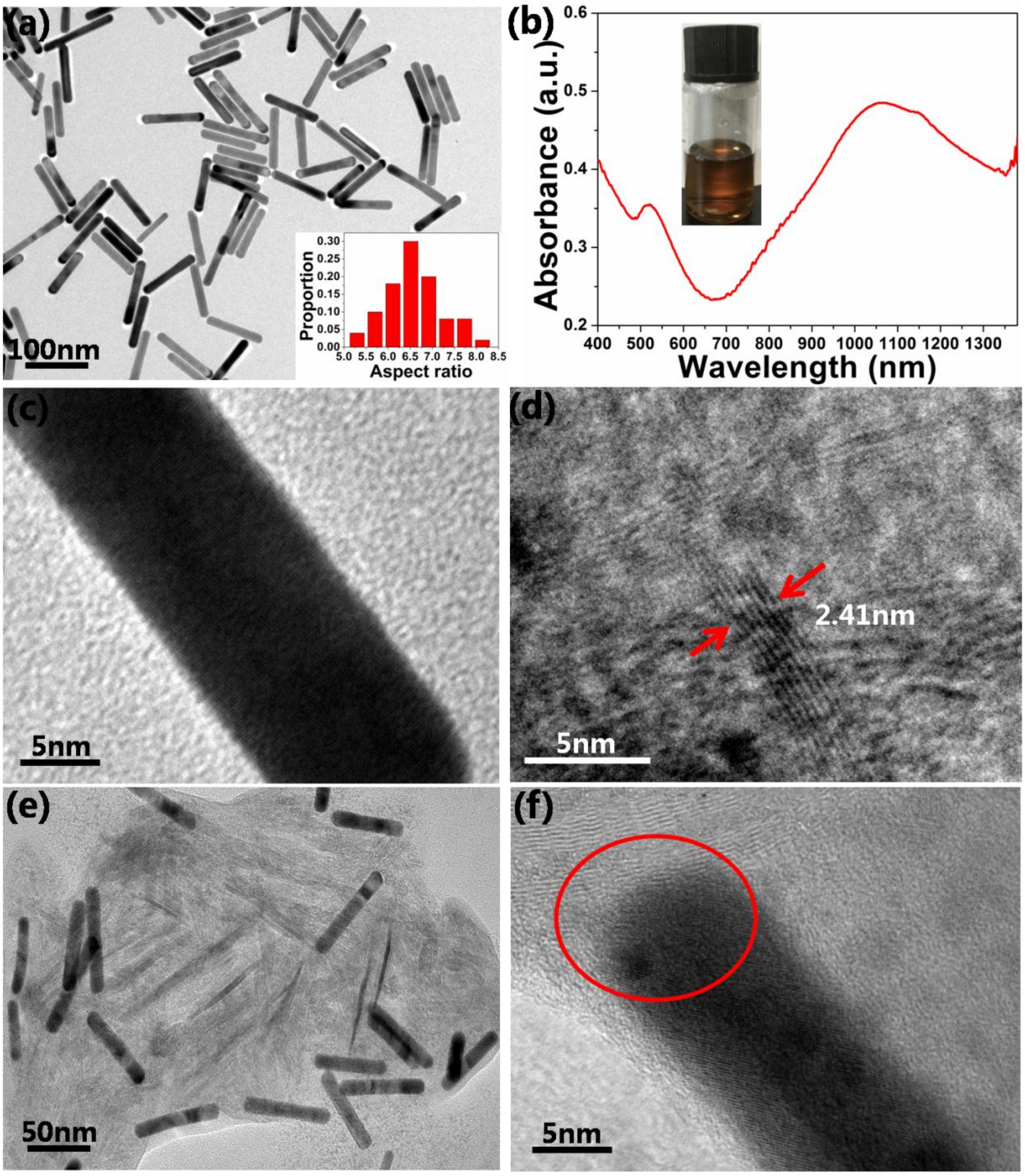

Fig. 3. (a) TEM image and aspect ratios distribution of the GNRs. (b) UV-Vis absorption spectra and photograph of the aqueous solution of GNRs. (c) HRTEM image of the GNRs. (d) HRTEM image of the graphene films. (e) TEM image of the G@GNRs nanocomposites. (f) HRTEM image of the G@GNRs nanocomposites.

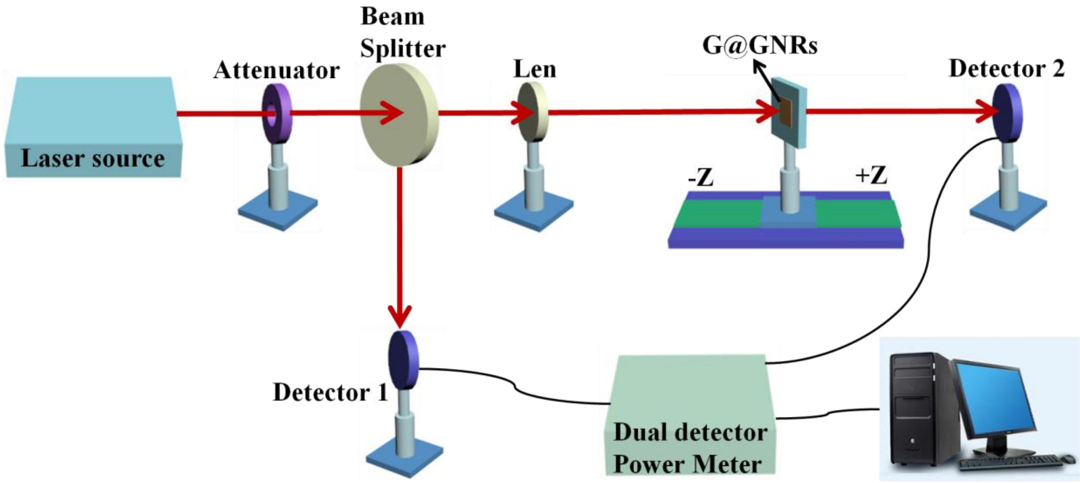

Fig. 4. The experimental setup of open-aperture Z-scan technique at 1064 nm.

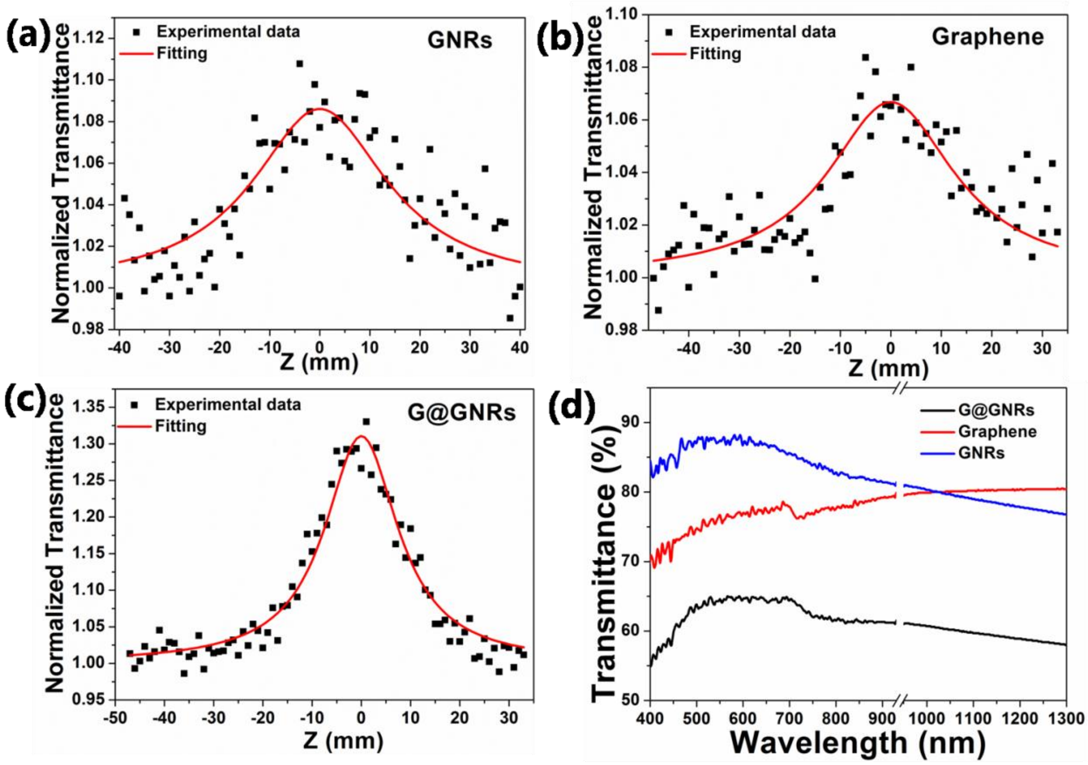

Fig. 5. The experimental results and fittings measured by Z-scan technique at 1064 nm. The open-aperture Z-scan curves for (a) GNRs, (b) graphene and (c) G@GNRs, respectively. (d) The linear optical transmittance of GNRs, graphene and G@GNRs.

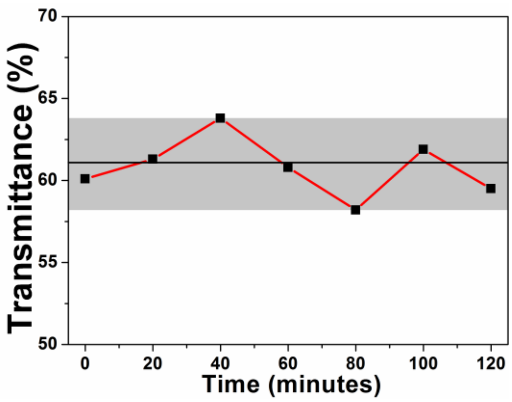

Fig. 6. The the opitcal transmittance was measured every 20 minutes at 1064 nm wavelength.

Material	α_0 (cm^{-1})	β (cm/GW)	T (%)	$\alpha_0 L$ (%)	I_s (GW/cm^2)
GNRs	2.3×10^5	-1.01×10^5	79.4	23	6.55
Graphene	9.1×10^5	-3.24×10^5	80.1	22	8.55
G@GNRs	4.1×10^5	-3.39×10^5	60.1	51	6.23

Table 1. Nonlinear optical parameters of the GNRs, graphene and G@GNRs obtained from the experimental data by using equation (1) and (2). α_0: the linear absorption coefficient; β: the nonlinear absorption coefficient; T: the linear transmittance at 1064 nm; $\alpha_0 L$: modulation depth; I_s: saturable intensity.